Changing Climate: Geothermal Evidence from Permafrost in the Alaskan Arctic

ARTHUR H. LACHENBRUCH AND B. VAUGHN MARSHALL

Temperature profiles measured in permafrost in northernmost Alaska usually have anomalous curvature in the upper 100 meters or so. When analyzed by heat-conduction theory, the profiles indicate a variable but widespread secular warming of the permafrost surface, generally in the range of 2 to 4 Celsius degrees during the last few decades to a century. Although details of the climatic change cannot be resolved with existing data, there is little doubt of its general magnitude and timing; alternative explanations are limited by the fact that heat transfer in cold permafrost is exclusively by conduction. Since models of greenhouse warming predict climatic change will be greatest in the Arctic and might already be in progress, it is prudent to attempt to understand the rapidly changing thermal regime in this region.

DURING THE LAST DECADE OR SO, THERE HAS BEEN A growing interest in the impact of human activities on the global composition of the atmosphere and its likely effect on climate. Because of the great social, economic, and scientific importance of such anthropogenic climatic changes, they are being intensively studied in order to derive predictive models. Most current models indicate that by the middle of the next century, the global mean air temperature near the ground should increase a few Celsius degrees, with the effects accentuated in the Arctic (*1*). Although "predicted temperature changes should be detectable by now" (*2*, p. 23), such changes have not been clearly identified in the recorded meteorological data (*3*). The most studied database is the surface air temperature, which shows large variability in time and space on all scales, with few records in the Arctic extending back far enough to put the effects of the modern carbon dioxide buildup in the context of climatic changes known to occur on longer time scales.

Unlike air temperatures, which depend on a thermal environment that changes hourly, temperatures beneath the ground surface in cold permafrost represent a systematic running mean of the recent temperature history at the surface; they are unaffected by thermal complications from moving fluids. Because a temperature change at the surface takes time to propagate downward into the earth, the deeper the temperature measurement, the farther back in time is the interval of surface temperature history that it represents and the smoother is the signal as the high-frequency noise is progressively filtered out. Thus the ground "remembers" the major events in its surface temperature history, and careful temperature measurements made today to depths of a few hundred meters can provide information on the history of local surface temperature during the past few centuries (Fig. 1). These methods have been illustrated with data from continuous permafrost at three widely separated points along the Alaskan Arctic Coast: Barrow (SB3 in Fig. 2) (*4*), Cape Thompson (CTD in Fig. 2) (*5*), and Prudhoe Bay (Fig. 2) (*6*). In this article, we present data showing that the dramatic warming of the last century recorded in the permafrost at these coastal sites is characteristic of much of a 10^5-km^2 region extending inland to the Brooks Range. Whether these changes are related to anthropogenic climatic factors is not within the scope of this discussion. However, the geothermal data suggest a substantial change in the heat balance at the surface of permafrost on a multidecade scale, a change that is occurring where early warnings of anthropogenic effects might be expected.

Overview of the Geothermal Regime

We obtained our data from oil exploration wells distributed throughout an area of rolling foothills and lake-strewn coastal plain between Alaska's Brooks Range and the Arctic Ocean (Fig. 2). The major features of the temperature observations in these wells and their interpretation in terms of heat-conduction models can be illustrated by the data from Awuna, a site in the Foothills province 150 km from the Arctic Coast (AWU in Fig. 2) (*7*). For temperatures measured at three successive times after the completion of drilling (Fig. 3A), the temperature becomes colder at each depth as the heat introduced by drilling dissipates. Figure 3B shows that this cooling follows the simple heat-conduction model for a line source of finite duration in an infinite homogeneous medium (*4*, *8*); for this case, successive temperature measurements fall on a straight line when plotted in the manner shown in Fig. 3B. The right-hand ordinate line in Fig. 3B represents infinite time, and a short extrapolation to it yields the equilibrium (before drilling) temperature with confidence; it is plotted (by dots) in Fig. 3A. In Fig. 4, the upper portion of the latest Awuna profile, corrected for the drilling disturbance (~0.9°C), is plotted with the preceding reading in the correct relative position for reference.

The linear portion of the profile at depth in Fig. 4 represents steady flow of heat q from the earth's interior according to the Fourier relation

$$q = K\Gamma_0 \qquad (1)$$

where Γ_0 is the thermal gradient and K is thermal conductivity. Extrapolation of the linear portion to the surface yields the intercept temperature θ_0. Our main interest is in the upper 100 m or so and the curvature there that causes a warming departure of the geotherm from the extrapolated linear profile; the resulting temperature anomaly (stippled area in Fig. 4) is denoted by $T(z)$. In the simplest interpretation $T(z)$ represents the response of the ground to recent warming of the mean annual surface temperature from a previous

The authors are geophysicists with the Office of Earthquakes, Volcanoes, and Engineering, U.S. Geological Survey, Menlo Park, CA 94025.

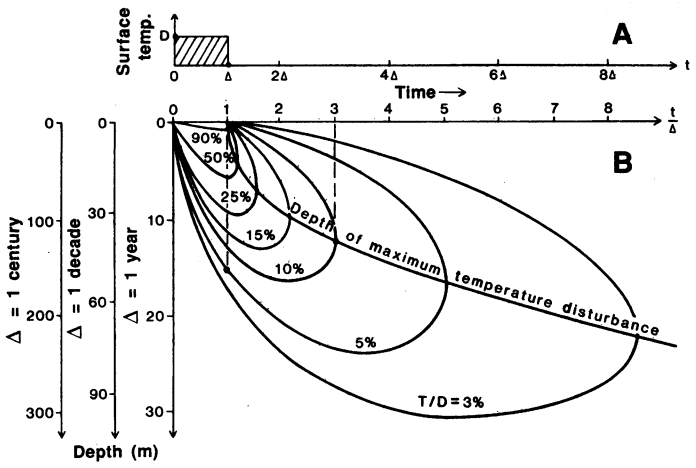

Fig. 1. The thermal memory of the earth for events on its surface. A uniform temperature anomaly of duration Δ at the surface (A) propagates downward and fades away as shown in (B). Curves show strength of the temperature anomaly T in the depth-time field expressed as a percentage of anomalous surface temperature D. The ordinate scales give depth in meters for events with durations of 1 year, 1 decade, and 1 century, respectively, for an assumed thermal diffusivity ($\alpha = 10^{-6}$ m^2 sec^{-1}). Two event-durations after the conclusion of an event (that is, at $t = 3\Delta$), the maximum signal falls to 10%, and it occurs at about 11 m for Δ = 1 year and 110 m for Δ = 1 century. At the conclusion of a uniform disturbance of duration Δ, the anomaly is not appreciable (<5%) below about 50 m for Δ = 1 decade, and about 150 m for Δ = 1 century.

long-term value of θ_0; the gradient reversal above the circled dot could represent a very recent cooling. This interpretation is illustrated in Fig. 5B for a simple hypothetical temperature history shown in Fig. 5A. [The theory of such changes has been widely discussed (*9–11*).]

The configuration of the geotherm at Awuna is not unique (Fig. 6). In fact, Figs. 6 to 9 (representing all stations shown in Fig. 2) show that most sites display a similar warming anomaly $T(z)$ (stippled areas), although irregularities can make the anomaly difficult to evaluate or, in extreme cases, to identify. In Figs. 6 to 9, the curves are offset to display their form; consequently, the intercept value at the surface, θ_0, does not appear. The individually estimated values of θ_0 are shown and contoured in Fig. 2. The fact that they can be contoured in this simple manner—values increase systematically with distance from the coast in a pattern modified by regional topography—supports the interpretation of θ_0 as a long-term mean surface temperature with regional climatic significance.

Departures from the Simple Model

It is useful to look more carefully at the possible departures from the foregoing model of one-dimensional transient conductive heat flow in a homogeneous medium. Even though the cold permafrost

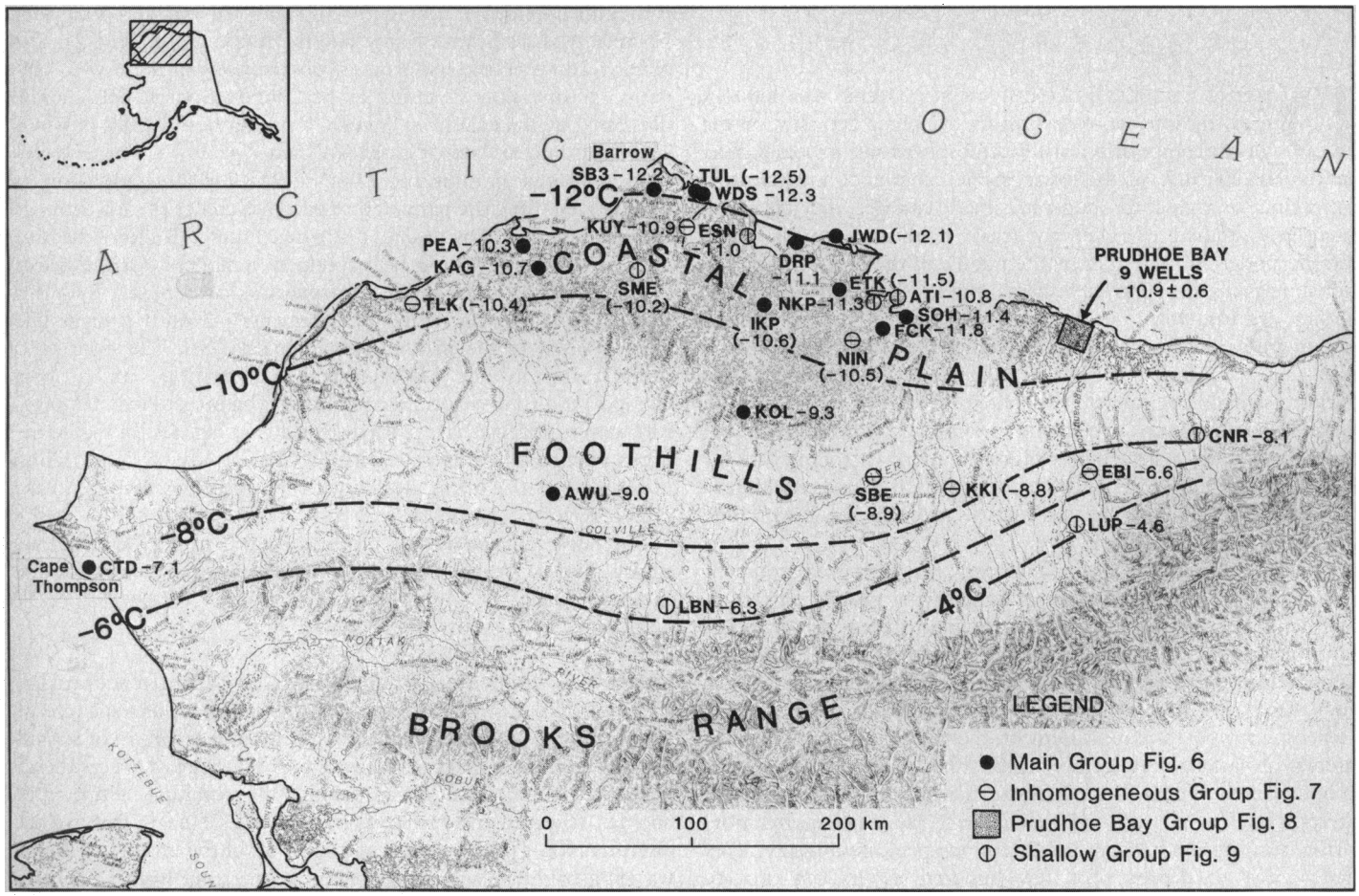

Fig. 2. Map of northern Alaska showing well locations with symbols keyed for Figs. 6 to 9. All except the "shallow group" indicate surface warming over a period of several decades to a century. Numbers and contours (dashed curves) represent the extrapolated long-term mean annual temperature at the top of permafrost, θ_0.

permits us to neglect heat transport by moving ground water and to treat this as a problem in heat conduction, other interpretations of the departure from the straight-line profile in the stippled regions illustrated (Figs. 4 and 6 to 9) are theoretically possible.

The governing equation for time-dependent two-dimensional heat flow in an inhomogeneous medium is

$$\frac{\partial}{\partial z} K\frac{\partial \theta}{\partial z} + \frac{\partial}{\partial y} K\frac{\partial \theta}{\partial y} = \rho c\frac{\partial \theta}{\partial t} \quad (2)$$

where θ is temperature, t is time, ρc is volumetric heat capacity, and K is thermal conductivity, treated generally as a function of position. Distance downward from the permafrost surface is z, and y is a horizontal coordinate; the third space coordinate is not needed. Manipulation of Eq. 2 yields an expression for the curvature in the temperature profile

$$\frac{\partial^2 \theta}{\partial z^2} = \frac{\rho c}{K}\frac{\partial \theta}{\partial t} - \frac{1}{K}\frac{\partial}{\partial y} K\frac{\partial \theta}{\partial y} - \frac{1}{K}\frac{\partial K}{\partial z}\frac{\partial \theta}{\partial z} \quad (3)$$

In the simple interpretation, we assumed that the second and third terms on the right in Eq. 3 (representing horizontal temperature variation and vertical inhomogeneities, respectively) vanished and that curvature of the temperature profile was given by the transient term (the first term on the right). Figure 10 illustrates a case in which the curvature might be explained by the second term on the right, and Fig. 11 by the third term. In Fig. 10, the curvature results from drilling in an anomalously warm place, such as a shallow lake. In this case, θ_0 would still represent the predominant regional long-term mean annual temperature. Figure 11 shows the important role of inhomogeneity represented by the last term on the right in Eq. 3; with the other two right-hand terms neglected, Eq. 3 reduces to

$$K\frac{d\theta}{dz} = \text{constant} \quad (4)$$

A systematic upward increase in conductivity might cause a systematic upward decrease in gradient and simulate the transient warming

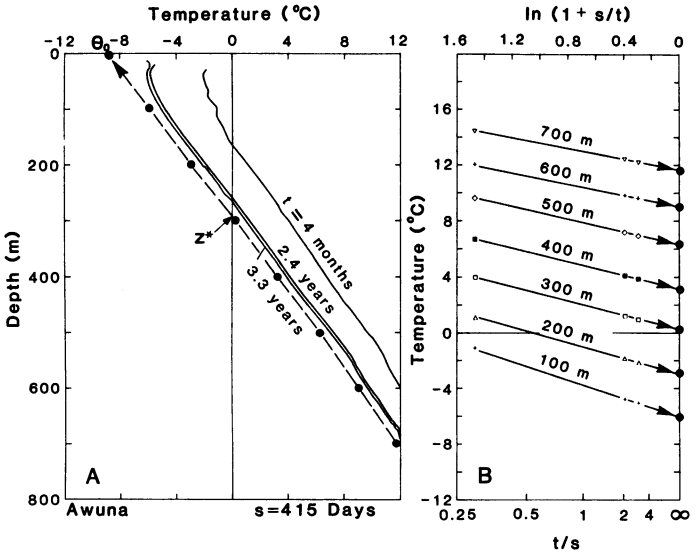

Fig. 3. (A) Successive temperature profiles from AWU observed at times t from 4 months to 3.3 years after completion of drilling of duration s = 1.14 years. Dots represent estimates of undisturbed temperature determined from (B); z^* is estimated permafrost depth and θ_0 is long-term mean surface temperature. (B) Representation of the dissipation of the drilling disturbance for the selected depths indicated; t is time elapsed since completion of drilling and s is duration of the drilling period. Extrapolated intercept at right-hand margin is equilibrium temperature.

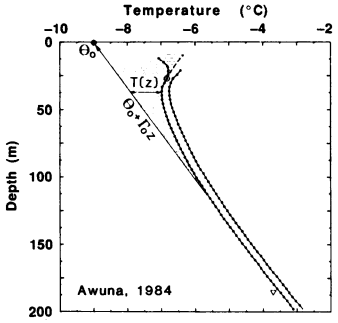

Fig. 4. Upper portion of latest measured profile at AWU, corrected for drilling disturbance, shown with previous measured profile in correct relative position. Line with slope Γ_0 and surface intercept θ_0 is least-squares fit to the linear portion of profile. $T(z)$ (stippled region) is temperature anomaly identified with a recent secular increase in surface temperature. Dots show every tenth measurement point; their diameter (~0.05°C) is the estimated reproducibility.

effect; for this case the extrapolated value θ_0 would have no simple physical meaning.

Three-dimensional effects (Fig. 10) exist in this terrain (*12*), and they must contribute to the anomaly $T(z)$ and add to the scatter of estimates for climatic change based on $T(z)$. However, the uniformity of sign of the observed $T(z)$, generally a warming, and the contourability of θ_0 (Fig. 2) suggest that these effects are secondary; the sites were not drilled selectively on lakes or topographic highs. For similar reasons, it is unlikely that the warm regions (stippled areas) are caused exclusively by conductivity contrasts; no evidence exists for a systematic increase in conductivity in the upper 100 m. In wells like Awuna (Fig. 4) and most of those illustrated in Fig. 6, the uniformity of gradient at depth permits linear extrapolation to the surface with reasonable confidence that K is uniform and therefore $T(z)$ is truly a transient anomaly. Profiles with less uniform gradients indicate contrasts in conductivity, and for them it is often difficult, in the selection of Γ_0, to distinguish between slope changes caused by climatic change and those caused by conductivity change (see, for example, ETK in Fig. 6 and Fig. 11). Gradual slope change at greater depth caused by conductivity changes could be confused with older climatic events. These ambiguities could be resolved positively if the thermal properties were known as a function of depth, but we do not have such information for most of the wells. Nevertheless, it seems clear from inspection of the profiles (Figs. 6 to 9) and from the foregoing discussion that the rather consistent departure from linearity toward warmer temperatures generally represents a transient warming. Where the gradient actually reverses sign (for example, at Awuna), the transient warming is the only plausible explanation.

Analysis of the Warming Anomaly

If $T(z)$ represents the effect of a recent warming of the surface, then the area between the curves defining $T(z)$ (stippled region in Fig. 4) gives a measure of the total amount of heat, Q, retained by a column of earth during the warming event

$$Q = \int_0^Z \rho c T(z)\, dz \quad (5)$$

where Z is the depth to which the anomalous temperature extends. The volumetric heat capacity, ρc, for all solid earth materials including ice is about the same (~0.5 cal cm^{-3} K^{-1}), permitting Q to be estimated from a knowledge of the size of the integrated anomaly $T(z)$. Whether this heat was absorbed slowly over a long time or rapidly over a short time must be determined by the form of $T(z)$; in the first case the anomaly would, of course, extend to greater depth Z. Thus the history calculation, that is, the estimate of the surface temperature change as a function of time involves two additional considerations: (i) the shape of $T(z)$ and (ii) the rapidity

with which the ground can conduct heat, which introduces the parameter K, more difficult to estimate than ρc in Eq. 5 (*13*).

Inhomogeneities and three-dimensional effects limit our capacity to resolve details of $T(z)$, and the lack of samples requires us to estimate thermal conductivity. Nevertheless, simple direct calculations based on the homogeneous one-dimensional transient model discussed provide insight into time scales and the general magnitude of temperature changes probably involved in generating the observed anomalies. For this purpose, we write the temperature (Fig. 4)

$$\theta = \theta_0 + \Gamma_0 z + T(z, t) \tag{6}$$

and substitution in Eq. 3 yields

$$\frac{\partial^2 T}{\partial z^2} = \frac{1}{\alpha}\frac{\partial T}{\partial t} \tag{7}$$

where $\alpha = K/\rho c$ is thermal diffusivity.

We assume that the surface temperature varies with time according to a simple three-parameter power law

$$T(0, t) = D\left(\frac{t}{t^*}\right)^{\frac{n}{2}} \text{ for } 0 < t \leqq t^* \text{ and } n = 0, 1, 2, \ldots \tag{8}$$

This provides the surface boundary condition for the solution of Eq. 7. The initial condition is

$$T(z, t) = 0 \tag{9}$$

The solution of Eqs. 7, 8, and 9 evaluated at $t = t^*$ is (*6, 14*)

$$T(z) = D\, 2^n\, \Gamma\left(\frac{1}{2}n + 1\right) i^n\text{erfc}\, \frac{z}{\sqrt{4\alpha t^*}} \tag{10}$$

where i^nerfc β is the nth integral of the error function of β (*14*, appendix II) and $\Gamma(\beta)$ is the gamma function of argument β. This result gives the ground temperature at the end of a surface warming interval of duration t^* during which the surface temperature increased by D. The form of the increase can be adjusted with the value n; $n = 0$ is a step increase in temperature, and $n = 2$ is a linear increase (Eq. 8).

Our general procedure has been to estimate and remove the linear part in Eq. 6 by fitting a least-squares line just below the curved upper portion (that is, above the triangle shown on each curve, Figs. 6, 8, and 9). The remaining anomaly $T(z)$ is fit to Eq. 8 by applying a linearized iterative least-squares procedure to obtain the parameters D and αt^* for various forms (n) of the surface temperature change. We generally assume that the diffusivity α is 10^{-6} m^2 sec^{-1}, so that we may discuss the result in terms of t^* in years. For other assumed or measured diffusivities, the result is easily adjusted.

An example of the best fitting results for Awuna for several values of n is shown in Fig. 12B. If the warming occurred as a step function ($n = 0$), it started about 40 years ago and warmed about 2 Celsius degrees; if it was a linear change ($n = 2$), the increase was 2.6 Celsius degrees during the last 68 years; an increase accelerating as the square of time ($n = 4$) would have started 97 years ago and grown to 2.9 Celsius degrees. It is convenient that the case $n = 1$ represents a step change in the rate of heat absorption by the earth (*14*). Such a change would have started 55 years ago and would have resulted in a temperature increase of 2.4 Celsius degrees and in a net annual heat absorption by the solid earth at the rate of 4 MJ m^{-2} year^{-1} (~0.14 W m^{-2}). The total heat absorption Q by the event, ~200 MJ m^{-2}, is about the same for all values of n because all solutions satisfy Eq. 5. Figure 12A shows that all four of the surface temperature histories illustrated in Fig. 12B fit the observations equally well, generally within the overall measurement error in the interval below 30 m where they were fit. The shallower observations (above the circled dot in Fig. 4) were not included because they represent a recent complication incompatible with the simple form of Eq. 8.

Although the Awuna example illustrates the ambiguity of historical details in this inverse method, it leaves little doubt that we are looking at the effects of a multidecade event in the last century that probably represents a temperature increase of 2 or 3 Celsius degrees. (Much of this ambiguity can be removed by careful long-term precision monitoring of the rate of temperature change versus depth.) The method is sensitive in the sense that this conspicuous disturbance to the earth's temperature was caused by the retention of only about 1% of the net radiation annually absorbed by the earth [~500 MJ m^{-2} year^{-1} in this region (*15*)]. This imbalance is too small to detect by direct measurements of the individual contributions to energy exchange at the earth's surface.

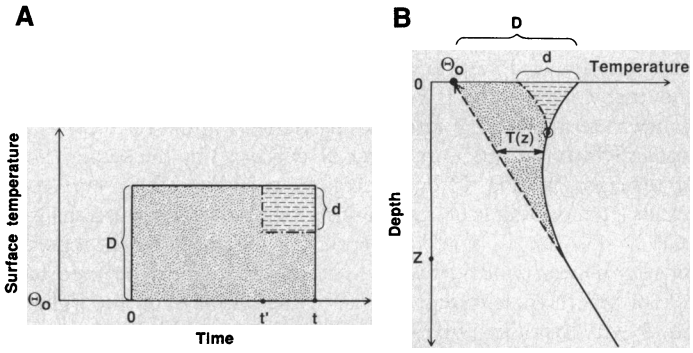

Fig. 5. Schematic representation of the effect of surface temperature history on the geotherm. A step increase in surface temperature in the amount D between time 0 and t [solid rectangle in (A)] results in departure of the upper part of the geotherm [solid curve in (B)] by $T(z)$ from the steady-state linear geotherm [dashed line in (B)]. A superimposed cooling in the amount d between t' and t [dash-dot line in (A)] would modify the geotherm as shown by the dash-dot curve above the circled point in (B).

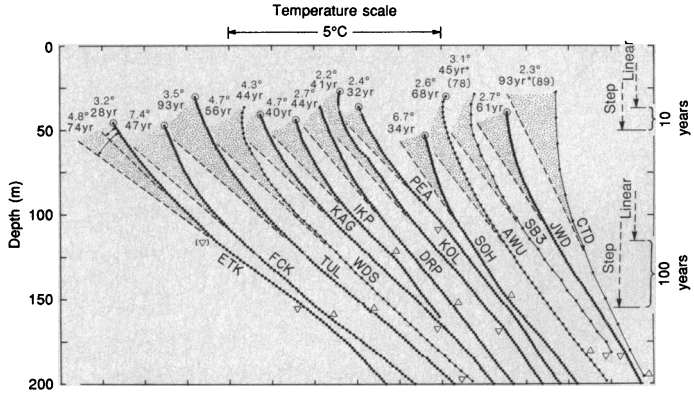

Fig. 6. Data from sites (denoted by ● in Fig. 2) with relatively smooth geotherms and indication of warming over several decades. Temperature origins are offset to avoid overlap. The stippled region for each curve is our interpretation of warming anomaly $T(z)$; numbers by curves indicate total temperature increase in Celsius degrees, and time in years before August 1984 for start-up in the best fitting model of linear change in surface temperature ($n = 2$, Eq. 8). Analyses performed on portion of each curve above the triangle, the region assumed to be homogeneous. Available shallow measurements have been deleted above circled dots for this analysis. Arrows at right-hand margin show depths at which step and linear changes in surface temperature, in progress for 10 or 100 years, become small (<5% of their surface value, assuming $\alpha = 10^{-6}$ m^2 sec^{-1}). Numbers in parentheses following asterisk are start-up times corrected for a diffusivity of 0.014 cm^2 sec^{-1} and a measurement date of 1961 for CTD, and for a measurement date of 1951 at SB3.

Application to Data from the Arctic Slope

We return now to the group of wells with temperature characteristics similar to the example at Awuna shown in Fig. 6. For each profile, $T(z)$ is a warming that extends to a depth of ~100 m, and, above the small triangles at least, each curve is generally smooth enough to permit a formal application of the foregoing analysis. For this purpose, we assumed that the surface temperature increased linearly with time ($n = 2$, Eqs. 7 to 10). The calculated temperature increase in Celsius degrees (D, Eq. 10) and the time in years before August 1984 since the start of the event (t^*, Eq. 10) are shown on the top of each curve. The effect on these parameters of using other forms of temperature history (that is, other values of n) can be judged from the example for Awuna (Fig. 12B). With one exception, the diffusivity was assumed to be 10^{-6} m^2 sec^{-1}; most of the values at sites in Fig. 6 are probably within ±25% of this, and extremes exceeding ±50% are unlikely. The exception is CTD, where measurements on the silicious siltstone core recovered from the hole in its natural frozen state yield an average diffusivity of about 1.4×10^{-6} m^2 sec^{-1} (Fig. 6).

One of the most uncertain results in Fig. 6 is that for ETK, which illustrates the problem of judging whether the change in slope at the point (∇) represents the base of the transient disturbance $T(z)$ or a steady-state effect of conductivity stratification; numerical results for both interpretations are shown. This major source of uncertainty and that due to unknown α could easily be removed with adequate core samples.

At the right-hand margin of Fig. 6, we show the depths beneath which effects of linear and step changes in surface temperature, in progress for 10 and 100 years, generally become difficult to observe (<5% of the surface temperature; see Fig. 1). It is clear from this reference alone that the duration of warming was much more than a decade but not much more than a century. Most of the numerical results from Fig. 6 lie in the range of 2 to 4.5 Celsius degrees for the warming and 40 to 90 years for the duration.

The estimate of start-up of the surface change, t^*, depends not only on the depth Z of $T(z)$ but also on the form and magnitude of $T(z)$. Those sites that indicate unreasonably large temperature changes (for example, FCK and SOH in Fig. 6) may have departures from the simple interpretative model that would make their value of t^* suspect as well.

The six profiles illustrated in Fig. 7 show variations in gradient that can be explained in these precision measurements only by stratification of thermal conductivity. Although these profiles are not amenable to the foregoing analysis, they all suggest a warming trend in the upper 100 m that is consistent with results in Fig. 6.

For comparison with Fig. 6, Fig. 8 shows the individual results for the nine drill holes at Prudhoe Bay that were analyzed (in an average sense) elsewhere (*6*). As these measurements were made in 1973, the value of t^* shown should be adjusted by 11 years for comparison with the later measurements just discussed. Although these curves are quite irregular, the results are fairly consistent in indicating an increase in surface temperature of 2 to 3 Celsius degrees starting more than a century ago if it was a linear change.

Results from the final seven sites shown on the map of Fig. 2 are given in Fig. 9. Unlike the wells previously discussed, none of these sites show evidence for a temperature anomaly extending deeper than 50 or 60 m. Three of the sites, NKP, ESN, and ATI, show a warming (below the circled points on profiles), which suggests a start-up about two decades ago when we use the previous assumptions. These wells show a transient cooling trend (above the circled dots), probably an event of the last decade, that is discussed in the next section. The profile at SME is unique for the Coastal Plain and Foothills provinces in showing only the recent cooling (above the

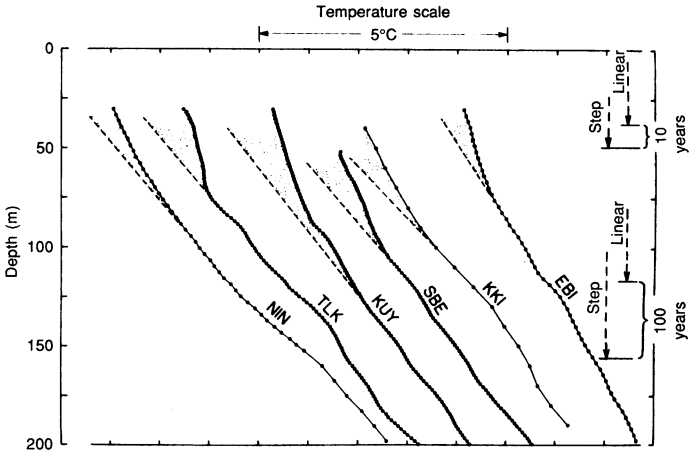

Fig. 7. Sites (denoted by ⊖ in Fig. 2) at which a variable gradient caused by conductivity contrasts precludes a confident identification of $T(z)$. Interpretations (dashed lines and stippled regions), though arbitrary, indicate that these profiles are not inconsistent with the warming effects shown in Fig. 6.

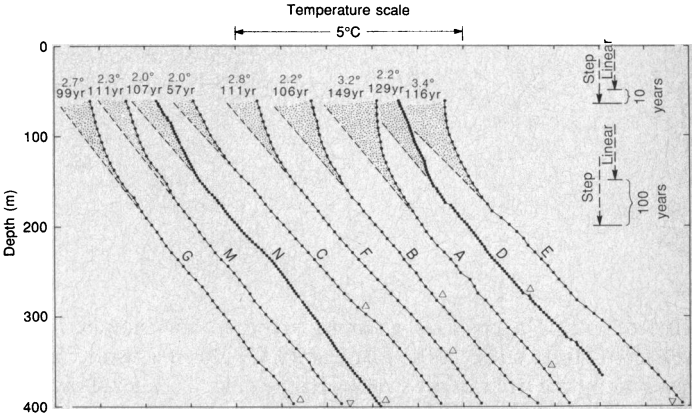

Fig. 8. Sites (contained in rectangle near Prudhoe Bay, Fig. 2) for which near-equilibrium (after drilling) profiles were available. Conventions are same as in Fig. 6, except analysis is based on a measured diffusivity of 1.6×10^{-6} m^2 sec^{-1}, and start-up times are measured in years before September 1973.

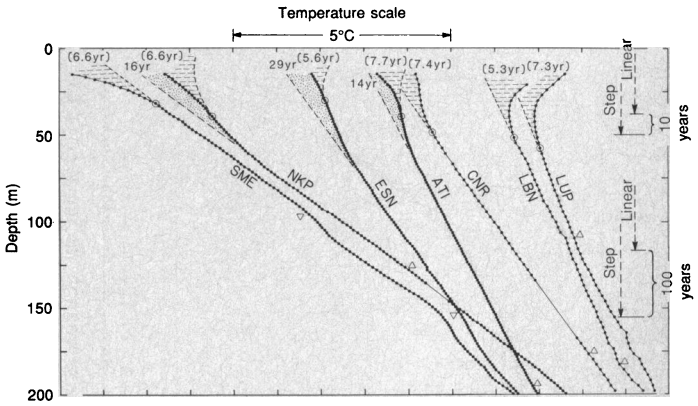

Fig. 9. Sites (denoted by ① in Fig. 2) with more superficial anomalies and little or no indication of multidecade warming. NKP, ESN, and ATI show recent warming [stippled area, $T(z)$] followed by a more recent cooling event indicated by the area between the dashed curve (extrapolated) and dots (measured). Circled dot on each curve is estimated limit of penetration of effects of the most recent event, a cooling at all sites except the three in the Brooks Range (CNR, LBN, and LUP). Numbers in parentheses give time in years between engineering modification of the surface and measurement of temperature profile.

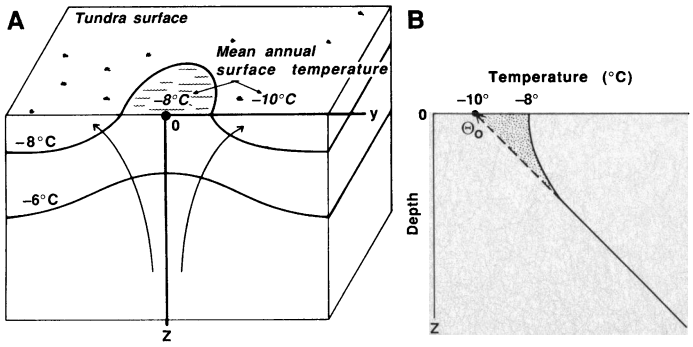

Fig. 10. Simulation of transient warming by steady-state three-dimensional heat flow. (A) Isotherms beneath an anomalously warm portion of the surface; the anomaly might be caused by standing water (illustrated) or blanketing by a hill. (B) Steady-state temperature profile (solid curve) for a well drilled at $y = 0$ in (A).

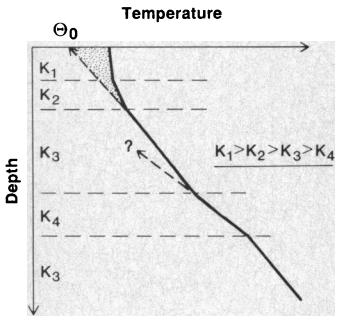

Fig. 11. Simulation of transient warming by one-dimensional steady-state flow in an inhomogeneous medium. Case illustrated is for conductivity decreasing progressively with depth. Steady-state gradient varies inversely with conductivity (Eq. 4).

circled point); a previous warming trend is not indicated. The remaining three sites, CNR, LBN, and LUP, form a distinct group lying along the front of the Brooks Range (Fig. 2). They show only a superficial warming trend (above the circled point) that may be largely a product of the last decade.

Consideration of Figs. 6 to 9, collectively, makes it clear that although our estimates for temperature change in the last century contain large uncertainties and the derived parameters do not show spatial trends that can be readily contoured, it would not be correct to treat these as random variations in a single population. The high quality of the data in Fig. 9 precludes the possibility of long-term warming indicated at most of the other sites, and the evidence suggests that warming at Prudhoe Bay might have started earlier than in some areas farther west and inland. The most reasonable conclusion is that although there was a fairly consistent warming trend of a few Celsius degrees at the permafrost surface during the last century in the Coastal Plain and Foothills provinces, it did not start at the same time throughout this region and probably did not extend into the Brooks Range. For comparison, air temperatures averaged throughout the Arctic indicate a warming from 1880 to about 1940 (fastest increase at about 1920), cooling until about 1970, and warming thereafter (*16*).

Events of the Last Decade

The temperature curves above the circles in Figs. 6 and 9 are curious. We believe they generally represent a recent change in permafrost surface temperature that was superimposed on the preexisting trend, as illustrated by the cooling *d* in Fig. 5. Such cooling is shown clearly at Awuna (Fig. 4) by the reversal in curvature at the circled point; this cooling trend had not penetrated to the measurement depths for the profile taken 11 months earlier. In Fig. 13, the observed profiles are extended upward beyond the circles where they had been truncated in Fig. 6. The dashed extensions of the curves in Figs. 13 and 9 are rough estimates of what the profile might have been in the absence of the recent cooling. We have shown in parentheses above these curves the number of years elapsed between the time of last measurement and the time the tundra surface was modified by the building of a construction pad before drilling. Sites with the younger pads generally seem to have shallower disturbances. Calculations with Eq. 10 show that these cooling disturbances are consistent with the assumption that they initiated with pad construction. This is seen in Fig. 14 where the estimated depth of the superimposed disturbance (that is, depth of circled points, Figs. 9 and 13) is plotted against age of the construction pad. The curves show the depth to which a step change ($n = 0$, Eq. 8) would no longer be detectable (<5% of its surface value, Fig. 1) for a plausible range of thermal diffusivities. Although a general climatic cause cannot be ruled out, Fig. 14 strongly suggests that modification of the surface for the drilling operation (a local disturbance) is responsible for the latest secular

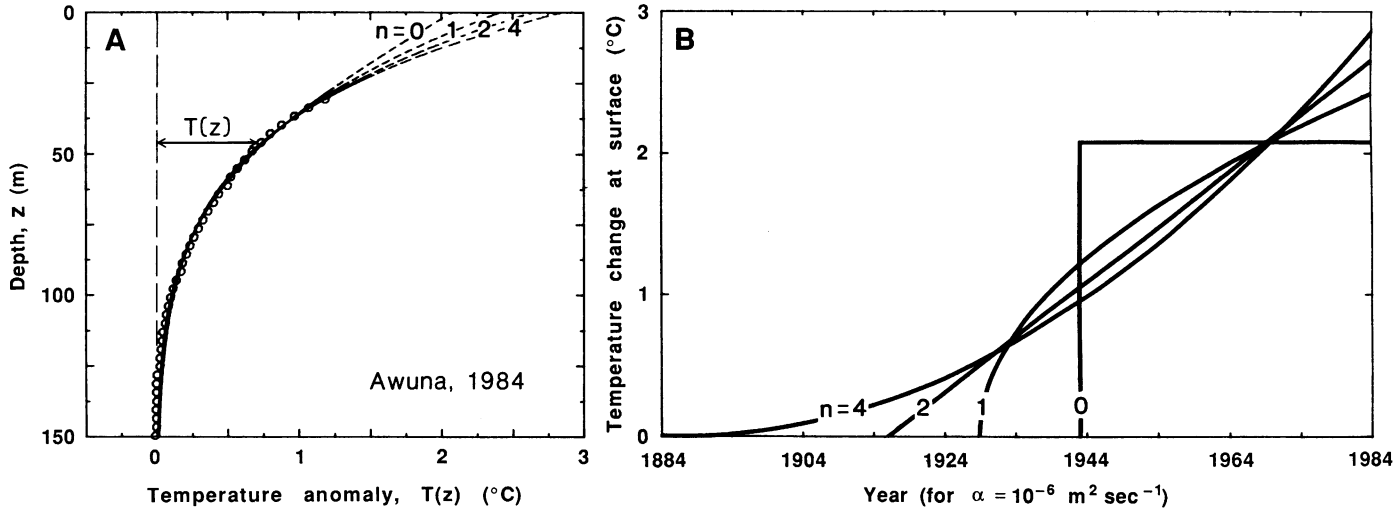

Fig. 12. (A) Warming anomaly $T(z)$ obtained from Fig. 4. Circles are observations; curves are best-fitting geotherms calculated by Eq. 10 for the four forms of temperature history shown in (B).

trend observed in permafrost surface temperature at these sites.

In the Coastal Plain and Foothills provinces, this recent trend is generally a cooling on the order of a degree or more; in some cases it is enough to nullify much of the climatic warming of the last century. Although we do not know the cause, we speculate that the slightly elevated, smooth, unvegetated construction pad might have a thinner drifted snow pack and less insulation from the winter cold than the surrounding terrain. Such effects can lower the mean ground temperature significantly (*17*). However, at the three sites (LBN, LUP, and CNR in Figs. 2 and 9) at the edge of the Brooks Range province, the recent event is a warming, which, according to its depth and age (Fig. 14), might also be caused by the engineering disturbance. The topographic setting and construction design were different for these sites, but we do not yet know enough to speculate on their thermal effects. Further study is needed of the long-range effects of these passive engineering modifications on the heat balance of the tundra surface. For the purpose of the present discussion, however, the observations underscore the sensitivity of permafrost temperature to modifications of the surface and the need to control these modifications near any observation wells that might be drilled to monitor long-term natural temperature changes.

Discussion

Our purpose is to point out some systematic temperature changes taking place in permafrost of the Alaskan Arctic so that they might be considered in the context of studies of contemporary climatic change. These changes are manifested as anomalous curvature in the upper 100 m or so of temperature-depth profiles. The anomalies can be interpreted confidently in terms of surface temperature history because of a special property of cold continuous permafrost: unlike most near-surface earth materials, it is unaffected by circulating ground water so that heat transfer within it is exclusively by conduction, a physically simple process. The "surface" whose temperature (T_{pf} in Fig. 15) is being analyzed is the upper surface of permafrost that lies beneath an annually thawing active layer whose thickness varies from 0.2 m in wet areas to 2 m in dry ones. This temperature differs from the "surface air temperature" obtained in a standard observatory thermometer shelter (T_{air} in Fig. 15) and frequently analyzed by climatologists (*3, 16*). It also differs from the mean temperature of the ground surface (T_{gs} in Fig. 15) or the mean for the solid surface (T_{ss} in Fig. 15) taken at the top of the snow pack when it is present or the ground surface when it is not. Between the top of permafrost and the air-temperature thermometer shelter, heat is transferred by radiation; by advection of sensible heat and of latent heat of fusion and vaporization; and by conduction, which in the active layer is generally associated with different transport and storage coefficients in the summer (thawed) and winter (frozen). We might generally expect a secular change in T_{air} to be reflected in a change in T_{pf} (*18*); the two quantities are usually within a few degrees of one another with the principal cause of difference probably being the seasonal snow pack. However, a tight correlation between the two quantities is hardly required in view of the complex and poorly understood regions (active layer, snow pack, and boundary layer) through which the two temperatures are coupled. Even our finding that changes in T_{pf} are not completely synchronous or readily represented by contours across the Alaskan North Slope might not be surprising in view of these complexities and their possible geographic variations. In any case, however, we expect that secular change in the mean temperature at the surface of permafrost will generally represent secular change in the rate of exchange of heat and moisture between the atmosphere and ground surface, that is, changes in climatic processes, however complex and locally variable they may be. In this sense, the marked secular changes indicated in permafrost temperatures represent secular climatic change. (Nonclimatic origins for thermal changes on this scale—ecological, geomorphic, or tectonic—seem most unlikely.)

Even if we knew the history of temperature change at the top of permafrost precisely, identifying the probable climatic cause would be difficult because of the lack of understanding of the near-surface processes (*15, 19*). This fact added to the ambiguity of geothermal

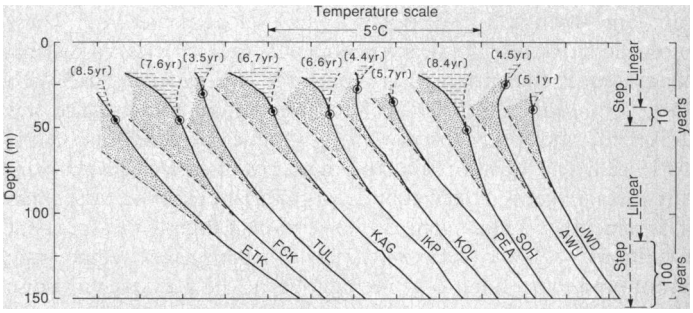

Fig. 13. Profiles of Fig. 6 including shallow measurements (above the dots) that show a recent cooling indicated schematically by the areas with dashes. Numbers in parentheses give time in years between engineering modification of the surface and measurement of temperature profile.

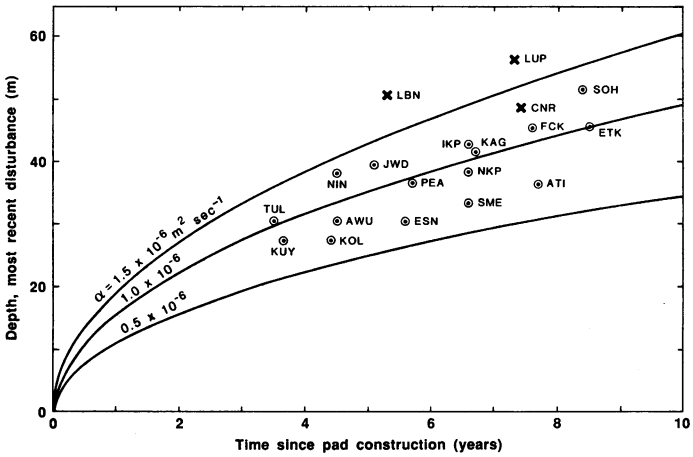

Fig. 14. Plot of estimated depth of penetration of most recent thermal disturbance (depth of circled dots, Figs. 6, 9, and 13) against age of construction pad at time of last observation. Curves show depths to which a step change in surface temperature at time of construction would penetrate for thermal diffusivities of $\alpha = 0.5 \times 10^{-6}$, 1.0×10^{-6}, and 1.5×10^{-6} m^2 sec^{-1}. Circles indicate a cooling disturbance; crosses, a warming disturbance.

Fig. 15. Measurement sites for the different annual mean temperatures: T_{pf} at upper surface of permafrost, T_{gs} at the ground surface, T_{ss} at the solid surface of the snow pack when it is present and ground surface when it is not, and T_{air} in a standard observatory thermometer shelter.

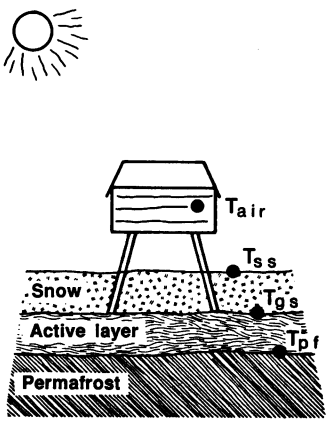

reconstructions of surface temperature, and the relative scarcity of geothermal data, probably explains why such data are not often considered in the search for documentation of contemporary climatic changes. In spite of the ambiguity of historical details, however, the data are robust indicators of the general time scale, the total heat absorbed by the earth, and the total temperature increase associated with the changes (Fig. 12A). The geothermal anomalies are sensitive to small departures from heat balance; in our examples, conspicuous surface temperature disturbances of a few Celsius degrees, detectable to a depth of 100 m in the earth, resulted from a net secular heat gain large enough to melt only a 1-cm layer of ice per year. These anomalies are direct physical consequences (not proxies) of thermal conditions at the surface. Their presence (for example, at AWU) leaves little doubt that the (permafrost) surface heat balance was disturbed, and their absence (for example, at SME) is strong evidence that it was not. Unlike time series of surface air temperature measurements, which contain large variations on all time scales and sometimes suffer from the effects of changing measurement conditions (*20*), the earth integrates the permafrost temperature uniformly and continuously, filtering out the (high-frequency) noise and preserving only the (low-frequency) signal. It is possible at any time to obtain climatic history information for the last century "after the fact" by drilling a 200-m observation well at any location where the information is desired.

Because of the filtering by the earth, long-term monitoring of future changes in critical areas could be carried out with infrequent (for example, yearly) measurements in carefully drilled and instrumented wells. Precision measurements over a time span of a decade or more will permit an analysis of the current rate of change as a function of depth in addition to the total change analyzed here. With the rate information, a much more precise reconstruction of the recent climate is possible from the earth-temperature record (*13*).

Conclusion

Throughout much of the 10^5-km^2 region of northernmost Alaska the temperature at the top of permafrost (0.2 to 2.0 m beneath ground surface) has generally increased about 2 Celsius degrees or more during the last several decades to a century. Details of the reconstruction are limited by the lack of information on thermal properties and, to a lesser extent, by the ambiguity of the inverse heat conduction problem. The start-up was not synchronous throughout this region, and its parameters are not readily contourable with existing data. Evidently, the warming started earlier in the Prudhoe Bay area than in some areas farther west and inland, and, if it reached our sites in the Brooks Range, it did so only in the last decade. A secondary result that deserves further analysis is the implication that temperature changes of a degree or more during the last decade resulted from the local passive modification of the surface caused by building construction pads before drilling. The long-term thermal effect of such structures on permafrost is a little-known subject of considerable interest.

The geothermal reconstruction of permafrost surface temperature has advantages and disadvantages as a means of studying contemporary climatic change. Advantages include the following: (i) The long-term signal of major events is preserved, and high-frequency noise is not. (ii) The measured anomaly is a direct thermophysical consequence of the thermal event under study, not a proxy. (iii) The information on surface temperature history can be recovered where and when it is desired (without real-time monitoring) by drilling an observation well. Disadvantages include the following: (i) Observations require a costly borehole, ideally with continuous core. (ii) Reconstructions of surface temperatures are inherently ambiguous in detail. (iii) The relation between permafrost surface temperature and routinely measured climatological parameters is not well understood.

Because continuous permafrost is well suited for the geothermal reconstruction of surface temperature, and because it occurs in the polar continental regions where anthropogenic climatic changes are expected to be largest and possibly first observable, it should be useful as a medium for studying such changes. Therefore, it is important to understand the presently changing thermal regime there, whether it is artificially induced or a background upon which such change will eventually be superimposed.

REFERENCES AND NOTES

1. National Research Council, *Carbon Dioxide and Climate: A Second Assessment* (National Academy Press, Washington, DC, 1982).
2. G. Weller, in *Proceedings, The Potential Effects of Carbon Dioxide–Induced Climatic Changes in Alaska*, J. H. McBeath, Ed. (School of Agriculture and Land Resources Management, University of Alaska, Fairbanks, 1984), pp. 23–30.
3. H. W. Ellsaesser, M. C. MacCracken, J. Walton, *Rev. Geophys. Space Phys.*, in press.
4. A. H. Lachenbruch and M. C. Brewer, *U.S. Geol. Surv. Bull. 1083-C* (1959), p. 79.
5. A. H. Lachenbruch, G. W. Greene, B. V. Marshall, in *Environment of the Cape Thompson Region, Alaska*, N. J. Wilimovsky and J. N. Wolfe, Eds. (Division of Technical Information, U.S. Atomic Energy Commission, Washington, DC, 1966), pp. 149–163.
6. A. H. Lachenbruch *et al.*, *J. Geophys. Res.* **87**, 9301 (1982). For other examples, see J. R. Mackay, *Energy Mines Res. Can. Geol. Surv. Pap. 75-1B* (1975), p. 173.
7. For more details on the thermal regime at each site, see A. H. Lachenbruch *et al.*, *U.S. Geol. Surv. Prof. Pap. 1399*, in press.
8. E. C. Bullard, *Geophys. Suppl. R. Astron. Soc. Mon. Notices* **5**, 127 (1947).
9. F. Birch, *Am. J. Sci.* **246**, 729 (1948).
10. V. Cermak, *Palaeogeogr. Palaeoclimatol. Palaeoecol.* **10**, 1 (1971).
11. T. E. Osterkamp, in *Proceedings, The Potential Effects of Carbon Dioxide–Induced Climatic Changes in Alaska*, J. H. McBeath, Ed. (School of Agriculture and Land Resources Management, University of Alaska, Fairbanks, 1984), pp. 106–113.
12. A. H. Lachenbruch *et al.*, in *Temperature—Its Measurement and Control in Science and Industry* (Reinhold, New York, 1962), vol. 3, pp. 791–803.
13. L. W. Gold and A. H. Lachenbruch, in *Permafrost: The North American Contribution to the Second International Conference* (National Academy Press, Washington, DC, 1973), pp. 3–23.
14. H. S. Carslaw and J. C. Jaeger, *Conduction of Heat in Solids* (Oxford Univ. Press, New York, 1959).
15. S. D. Dingman *et al.*, in *An Arctic Ecosystem: The Coastal Tundra at Barrow, Alaska*, J. Brown, P. C. Miller, L. L. Tieszen, F. L. Bunnell, Eds. (Dowden, Hutchinson & Ross, Stroudsburg, PA, 1980), pp. 30–71.
16. P. M. Kelly *et al.*, *Mon. Weather Rev.* **110**, 71 (1982).
17. A. H. Lachenbruch, *U.S. Geol. Surv. Bull. 1083-A* (1959), p. 1.
18. C. W. Goodwin, J. Brown, S. I. Outcalt, in *Proceedings, The Potential Effects of Carbon Dioxide–Induced Climatic Changes in Alaska*, J. H. McBeath, Ed. (School of Agriculture and Land Resources Management, University of Alaska, Fairbanks, 1984), pp. 92–105.
19. J. O. Fletcher and U. Radok, in *The Polar Regions and Climatic Change, Appendix* (National Academy Press, Washington, DC, 1984), pp. 1–32; C. R. Bentley *et al.*, *ibid.*, pp. 77–113; A. Judge *et al.*, in *Proceedings, Fourth International Conference, Permafrost* (National Academy Press, Washington, DC, 1984), pp. 137–138.
20. J. M. Mitchell, Jr., *Bull. Am. Meteorol. Soc.* **39**, 83 (1958).

21. We gratefully acknowledge comments on the manuscript from D. P. Adam, R. G. Barry, C. Benson, C. R. Bentley, J. Brown, H. W. Ellsaesser, J. O. Fletcher, B. L. Gartner, T. Hamilton, W. D. Harrison, J. R. Mackay, J. M. Mitchell, Jr., T. E. Osterkamp, J. H. Sass, C. Wahrhaftig, R. E. Wallace, A. L. Washburn, G. Weller, and J. H. Zumberge.